Ab initio Studies of the Band Parameters of III–V and II–VI Zinc-Blende Semiconductors[1]

S. Zh. Karazhanov and L. C. Lew Yan Voon^

Department of Physics, Worcester Polytechnic Institute, Worcester, Massachusetts 01609-2280, USA
^e-mail: llew@wpi.edu
Submitted November 5, 2003; accepted for publication May 17, 2004

Abstract—Electronic band-structure calculations are performed for zinc-blende III–V (AlP, AlAs, AlSb, GaP, GaAs, GaP, InP, InAs, and InSb) and II–VI (ZnS, ZnSe, ZnTe, CdS, CdSe, and CdTe) semiconductors using an ab initio pseudopotential method within a local-density approximation (LDA). Lattice parameters, band gaps, Luttinger parameters, momentum matrix elements and effective masses are studied in detail. It is shown that LDA calculations cannot systematically give accurate band parameters. It is found that LDA band parameters calculated using experimentally determined lattice constants are more accurate than those using LDA lattice constants. We found that inclusion of the *d* electrons of Group-II atoms in the core gives more accurate band parameters. © 2005 Pleiades Publishing, Inc.

1. INTRODUCTION

Density-functional theory (DFT) is a powerful tool for studying the electronic structure of solids. It is well known that the band gaps of bulk solids calculated within the theory are systematically underestimated compared to experimentally determined ones [1] because of the theory's failure to describe excited-state properties. Moreover, the problem rests with more than the local-density approximation (LDA). Following $\mathbf{k} \cdot \mathbf{p}$ theory (see, e.g., [2]), however, one can say that if fundamental excitation gaps are incorrect, then band dispersions should be as well. This realization has been used by Cardona *et al.* [3–6] in generating corrected band parameters (Luttinger parameters and spin splittings) for a number of semiconductors. Nevertheless, there remains some dispute regarding this issue [7]. For instance, in 1992, Fiorentini and Baldereshi [8, 9], using pseudopotential plane waves within the LDA, found that conduction-band masses (m_c) at point Γ were very close to experimental values for GaAs, AlAs, and Ge. However, the values of m_c found in [10] differ significantly from those determined experimentally for GaAs, GaSb, InP, and InAs. Similarly, the conduction-band effective masses calculated by Wang and Zunger [11] within the LDA agree well with experimental data for Si, while for CdSe the masses were not very accurate and a semiempirical modification led to somewhat better agreement. Kane [12], however, found that it was not possible to attain correct band gap and cyclotron masses in Si with a local static potential such as the LDA. Fairly good agreement with the experiment was obtained by Wang and Klein [13] for the conduction and valence band effective masses of GaP, GaAs, ZnS, and ZnSe using a linear combination of Gaussian orbit-

als within the LDA. A systematic study by Huang and Ching [14] of the effective masses for 32 semiconductors using a semi–ab initio technique shows much better agreement. Therefore, despite the importance of effective masses, the question of whether calculations within the LDA give correct effective masses is still open.

There is even less explicit research on the correctness of momentum matrix elements (E_p) calculated within the LDA, which are often claimed to be accurate. However, the validity of the statement has been less directly verified. The standard argument is that, in a pseudopotential approach, the pseudo–wave function has a very high overlap with the true wave function [11]. The value of E_p for GaAs calculated by Winkler [15], and Kageshima and Shiraishi [16] within the LDA is about ~1.7 times smaller than that determined experimentally [17, 18]. Kageshima and Shiraishi [16] concluded that wave functions calculated by the pseudopotential method lack a precise description around the atomic core regions. Furthermore, they suggested that momentum matrix elements cannot be directly estimated from these wave functions because the functions are smoother around the atomic cores, while the actual wave functions oscillate greatly. To fix the error, a core-repair term was added. By including the correction, significant improvement was indeed achieved for zinc-blende and wurtzite GaN. However, momentum matrix elements for polysilane, siloxene, and GaAs calculated with the correction and without it differ from each other by only 5.43, 3.0, and 1.8%, respectively. Wang and Zunger [11], however, had previously found a larger increase in the momentum matrix elements. To complicate matters further, Levine and Allan [19] found that, even within a scissors approximation, the velocity operator becomes renormalized.

---

[1]This article was submitted by the authors in English.

It should be noted that the correctness of the calculated and experimentally determined values of E_p is also being debated. Efros and Rosen [20], for example, concluded that Fu, Wang, and Zunger's calculation result of $E_p = 14.98$ eV for bulk InP using a direct diagonalization method [21] is smaller than the measured value 20.6 eV, which indicates an underestimation of the coupling between the conduction and valence bands and an overestimation of the influence of the remote bands. However, even the values of E_p extracted from the experiments have an intrinsic scatter. For bulk InP, for example, experimental values of E_p vary from 16.6 [22] to 20.7 eV [23]. Therefore, the question of whether the momentum matrix elements calculated by the LDA are correct is still open.

It should also be noted that the above-mentioned problems are relatively less studied in II–VI semiconductors, which have a cation d band inside the main valence band playing a significant role in their electronic structures [24–29]. In III–V semiconductors the d levels are several eV lower in their energy than the lowest sp valence band states [30]. So the effect of the d states on the electronic structure of III–V compounds can be disregarded. In earlier research, the strong p–d coupling in II–VI semiconductors has usually been taken into account by including the d electrons (i) in the core, but also including nonlinear core corrections for exchange and correlation, and (ii) in the valence complex [24–26], but keeping the s and p semicore electrons in the core. Currently, the description of p–d coupling is still being improved. Despite numerous studies, the question as to which of the approaches related to p–d coupling is correct and consistent with $\mathbf{k} \cdot \mathbf{p}$ band parameters is still open.

In this paper we provide the first systematic study of eigenvalues at Γ, X, and L; the Kane momentum matrix elements E_p and E_p' (defined as $2P^2/m_0$ in eV) corresponding to the fundamental direct p–s energy gap E_g and the p–p gap E_g' at point Γ; the conduction-band effective masses m_c^{001}, m_c^{011}, and m_c^{111}; the heavy-hole effective masses m_{hh}^{001}, m_{hh}^{011}, and m_{hh}^{111}; the light-hole effective masses m_{lh}^{001}, m_{lh}^{011}, and m_{lh}^{111}; and the Luttinger parameters γ_1^L, γ_2^L, and γ_3^L. Furthermore, we answer the question as to whether band parameters calculated within the framework of the LDA are correct.

2. COMPUTATIONAL DETAILS

2.1. Local-Density Approximation

Ab initio calculations were performed for III–V (AlP, AlAs, AlSb, GaP, GaAs, GaP, InP, InAs, and InSb) and some II–VI (ZnS, ZnSe, ZnTe, CdS, CdSe, and CdTe) semiconductors with a zinc-blende structure. We did not study the II–VI compounds HgS, HgSe, and HgTe, because it is well known that spin–

orbit coupling (which is not accounted for in this work) plays a significant role [24]. The unit cell considered consists of two atoms of Group-III (II) at (0, 0, 0) and an atom of Group-V (VI) at ($a/4$, $a/4$, $a/4$), where a is the lattice constant.

Ab initio pseudopotentials were generated using the Trouillier–Martins method [31]. We have considered s, p and d as valence states in order to build the pseudopotential for the atoms of Group-III and V using the p potential as the local potential, while s and d are taken as the nonlocal parts. We determined E_{cut} by requiring convergence of the total energy E_{tot}. For all the III–V semiconductors considered, $E_{cut} = 60$ Ry was used.

To study the II–VI compounds, s, p, and d states were considered as valence states. Pseudopotentials for Group-II atoms were generated in two ways: (i) including the d electrons, which are inside the valence shell, in the valence complex while keeping the semicore s and p states in the core, and (ii) including the d electrons in the core. For the latter case, we used $E_{cut} = 30$ Ry, and a nonlinear exchange correlation was added, which is known to give better agreement with experimental data [25]. For the former case, convergent results were obtained for $E_{cut} = 70$ Ry. The semicore d electrons of the III–V compounds were included in the core because, as discussed in Section 1, the energy level of the electrons arc far below the outermost sp levels [30] and the electrons are not expected to signifcantly affect the band structure of the compounds.

Band-structure calculations were performed using the PEtot code developed by L.-W. Wang [32], which uses the ab initio pseudopotential method within the LDA and neglects spin–orbit coupling. The Pulay–Kerker scheme was used for self-consistent potential mixing. In addition, g-space Kleinman–Bylander nonlocal pseudopotential implementations were used with a mask function scheme, without the need for preprocessing the pseudopotentials. The LDA exchange-correlation contribution was accounted for by means of Perdew and Zunger's parametrization [33] of the calculations by Ceperley and Alder [34]. The self-consistent solution of the one-electron Kohn–Sham equation was performed using a planewave pseudopotential algorithm [35].

The potential for the unit cell under consideration was found by performing self-consistent calculations using 10 special k points in the Brillouin zone. Then, using this potential, eigenenergies at the special k points were found by nonconsistent calculations.

2.2. Band Parameters

Carrier effective masses are defined as

$$\frac{1}{m_c(\mathbf{k}_0)} = \frac{1}{\hbar^2} \frac{\partial^2 E(\mathbf{k})}{\partial k^2}\bigg|_{\mathbf{k} = \mathbf{k}_0} \tag{1}$$

Table 1. Experimental [37–40] and LDA (a_0, ad_0) lattice constants (Å) for the zinc-blende III–V and II–VI semiconductors with d electrons of Group-II atoms included in the core (a_0) and in the valence complex (ad_0)

	AlP	AlAs	AlSb	GaP	GaAs	GaSb	InP	InAs	InSb
a_0	5.4131	5.6246	6.0788	5.2836	5.5073	5.9380	5.6591	5.8564	6.2863
Experiment [39]	5.4670	5.6600	6.1355	5.4512	5.6533	6.0959	5.8687	6.0583	6.4794

	ZnS	ZnSe	ZnTe	CdS	CdSe	CdTe
a_0	4.8674	5.1706	5.6730	5.3038	5.5639	6.0517
ad_0	5.3404	5.6202	6.0072	5.8064	6.0572	6.4174
Experiment [37]	5.4102	5.6676	6.1037	5.8180	6.0520	6.4860
Experiment [38]	5.4110	5.6690	6.0890	5.8300	6.0840	6.4800
Experiment [40]	5.4100	5.6680	6.1000	5.8250	6.0520	6.4820

for a direction **k** about some point $\mathbf{k}_0$ in the Brillouin zone. We studied effective masses along [001], [011] and [111] directions in the vicinity of $\mathbf{k}_0 \equiv \Gamma(0, 0, 0)$ point. The masses can, in principle, be calculated by the $\mathbf{k} \cdot \mathbf{p}$ theory equation (see, e.g., [2]). In this study, we calculated the band energies at a sequence of k points around Γ and calculated m_c directly from Eq. (1).

We considered the conduction-band effective masses m_c^{001}, m_c^{011}, and m_c^{111}; the heavy-hole effective masses m_{hh}^{001}, m_{hh}^{011}, and m_{hh}^{111}; and the light-hole effective masses m_{lh}^{001}, m_{lh}^{011}, and m_{lh}^{111}. To calculate the effective masses, 11 k points were used in the ranges from $(2\pi/a)/(0, 0, -1/20)$ to $(2\pi/a)/(0, 0, 1/20)$ for the direction [001], from $(2\pi/a)/(0, -1/20, -1/20)$ to $(2\pi/a)/(0, 1/20, 1/20)$ for the direction [011], and from $(2\pi/a)/(-1/20, -1/20, -1/20)$ to $(2\pi/a)/(1/20, 1/20, 1/20)$ for the direction [111]. The momentum matrix elements were determined at the Γ point.

Following [36] and using the calculated effective-mass values, the Luttinger valence-band parameters γ_1^L, γ_2^L, and γ_3^L were calculated as

$$\gamma_1^L = \frac{1}{2}\left(\frac{1}{m_{lh}^{001}} + \frac{1}{m_{hh}^{001}}\right), \qquad (2)$$

$$\gamma_2^L = \frac{1}{4}\left(\frac{1}{m_{lh}^{001}} - \frac{1}{m_{hh}^{001}}\right), \qquad (3)$$

$$\gamma_3^L = \frac{1}{4}\left(\frac{1}{m_{lh}^{001}} + \frac{1}{m_{hh}^{001}} - \frac{2}{m_{hh}^{111}}\right). \qquad (4)$$

Energies and momentum matrix elements are given in eV, and effective masses are given in units of the electron rest mass m_0 throughout the paper. All the calculations were performed for two values of the lattice constants: (i) determined experimentally (to be called the experimental lattice constant hereafter) and (ii) determined by a search of the total energy minimum (to be called the theoretical lattice constant hereafter).

3. RESULTS

3.1. Lattice Constants

It will become clear that band structure depends critically upon such parameters as the lattice constant (among others). By a search of the total-energy minimum, lattice constants were found (Table 1) that, for the III–V compounds and II–VI semiconductors with d electrons included in the valence complex, differ from those determined experimentally by <3 and <1.5%, respectively. However, if the d electrons of Group-II atoms are included in the core, then calculated lattice constants for the II–VI compounds differ significantly from experimentally determined ones (>7%). It should be noted that experimentally determined lattice constants for II–VI compounds given in handbooks differ somewhat from each other. For example, in [37], the lattice constant for CdSe is $a = 6.052$ Å while in another handbook, [38], $a = 6.084$ Å. Our calculated lattice constant is between the two experimental values. Since, for all the other semiconductors considered in this study, the calculated lattice constant is always smaller than the experimentally determined one, we used $a = 6.084$ Å for CdSe from [38] for band-structure calculations using the experimental lattice constant. For other II–VI compounds, we used the experimental lattice constants given in [37].

3.2. Eigenvalues

Self-consistent and nonconsistent band-structure calculations were performed using both calculated and experimentally determined lattice constants. As we disregarded spin–orbit coupling, the valence band maximum at point Γ is triple degenerated for all the compounds considered. For III–V and II–VI compounds, eigenvalues at Γ, X, and L are given in Table 2, and they are in general agreement with previous calculations [9, 13, 14, 24–26, 29, 41–43]. Band gaps (E_g) for AlP, AlAs, AlSb, and GaP are indirect, with the valence band maximum at point Γ and conduction band minimum at point X, while those for other III–V compounds are direct. As expected, band gaps for AlP, AlAs, AlSb,

Table 2. Eigenvalues (eV) at Γ, X, and L for the zinc-blende III–V and II–VI compounds calculated using the theoretical (a_0, ad_0) and experimental (a_e, ad_e) lattice constants including the d electrons of Group-II atoms in the core (a_0, a_e) and in valence complex (ad_0, ad_e). The results are compared to experimental data [39, 40] and theoretical calculations within $\mathbf{k} \cdot \mathbf{p}$ theory [2], LDA, and GW [25]

		AlP	AlAs	AlSb	GaP	GaAs	GaSb	InP	InAs	InSb
Γ_1^c	a_0	3.3457	2.1517	1.6488	2.5982	1.1885	0.5885	1.3831	0.4131	0.2986
	a_e	3.0929	1.9979	1.4354	1.7736	0.5337	0.0000	0.7205	0.0000	0.0000
X_1^c	a_0	1.4194	1.3127	1.1291	1.4058	1.2861	0.8275	1.5522	1.3821	1.2050
	a_e	1.4739	1.3437	1.1766	1.5872	1.4245	0.9086	1.7198	1.5340	1.3487
L_1^c	a_0	2.7809	2.1399	1.3611	1.9424	1.2413	0.5738	1.8019	1.2331	0.7186
	a_e	2.6692	2.0680	1.2806	1.6262	0.9888	0.3868	1.4918	0.9624	0.5300
Experiment [39]		3.6200	3.1400	2.2190	2.7800	1.4240	0.7500	1.3400	0.4180	0.1800
$\mathbf{k} \cdot \mathbf{p}$ [2]		5.1200	3.0600		2.8700	1.5200	0.8100	1.4200	0.4200	0.2370

		ZnS	ZnSe	ZnTe	CdS	CdSe	CdTe
Γ_1^c	a_0	5.325	3.908	2.971	3.646	2.780	2.186
	a_e	2.933	1.968	1.587	2.155	1.513	1.217
	ad_0	2.004	1.180	1.077	0.913	0.394	0.499
	ad_e	1.868	1.076	0.901	0.901	0.371	0.420
X_1^c	a_0	2.953	2.594	1.971	3.379	2.932	2.329
	a_e	3.618	3.171	2.451	3.757	3.322	−1.263
	ad_0	3.132	2.764	2.125	3.301	2.923	2.364
	ad_e	3.242	2.820	2.167	3.311	2.943	2.427
L_1^c	a_0	5.159	4.073	2.621	−0.487	4.003	2.750
	a_e	3.985	3.107	2.117	3.908	3.186	−0.462
	ad_0	3.128	2.395	1.610	2.770	2.193	1.605
	ad_e	3.084	2.351	1.563	2.761	2.179	1.581
Experiment [40]		3.680	2.700	2.280	2.500	1.900	1.490
$\mathbf{k} \cdot \mathbf{p}$ [2]		3.800	2.820	2.390	2.560	1.840	1.600
LDA [25]		2.370	1.450	1.330	1.370	0.760	0.800
GW [25]		3.980	2.840	2.570	2.830	2.010	1.760

GaP, GaAs, and GaSb calculated using both of the lattice constants are underestimated, while those for InP, InAs, and InSb are overestimated for the calculated lattice constant and underestimated for the experimentally determined lattice constant. The overestimate can be related to the small gap and the disregarding of the spin–orbit coupling; similar results were obtained by Huang and Ching [14]. One can also see that the LDA calculations of different authors vary significantly. For example, the direct band gap of GaAs, GaSb, InAs, and InSb calculated by Geller *et al.* [10] within the LDA using the full-potential linearized augmented plane-wave (FLAPW) method was 0.25, –0.3, –0.53, and –0.57 eV, respectively, while that of AlAs, GaAs, and GaSb calculated by Wei and Zunger [41] within the LDA was 1.84, 0.15, and –0.165 eV, respectively. The band gaps of III–V compounds that we calculated are similar to those of [8, 9, 15].

It should also be noted that the direct band gaps calculated in this study using the calculated lattice constant are larger than those found using the experimentally determined lattice constants. This can be attributed, in part, to the direct-gap increase with compression (equivalent to small a). In the latter case, band gaps can even be zero for GaSb, InAs, and InSb. Moreover, the band gaps for AlP, GaP, GaAs, GaSb, InP, InAs, and InSb calculated using the calculated lattice constants are much closer to the experimental band gaps.

For the II–VI compounds, the calculated eigenenergies are in general agreement with previous calculations [24–26]. If the d electrons of the atoms of Group-II are included in the core with nonlinear core corrections,
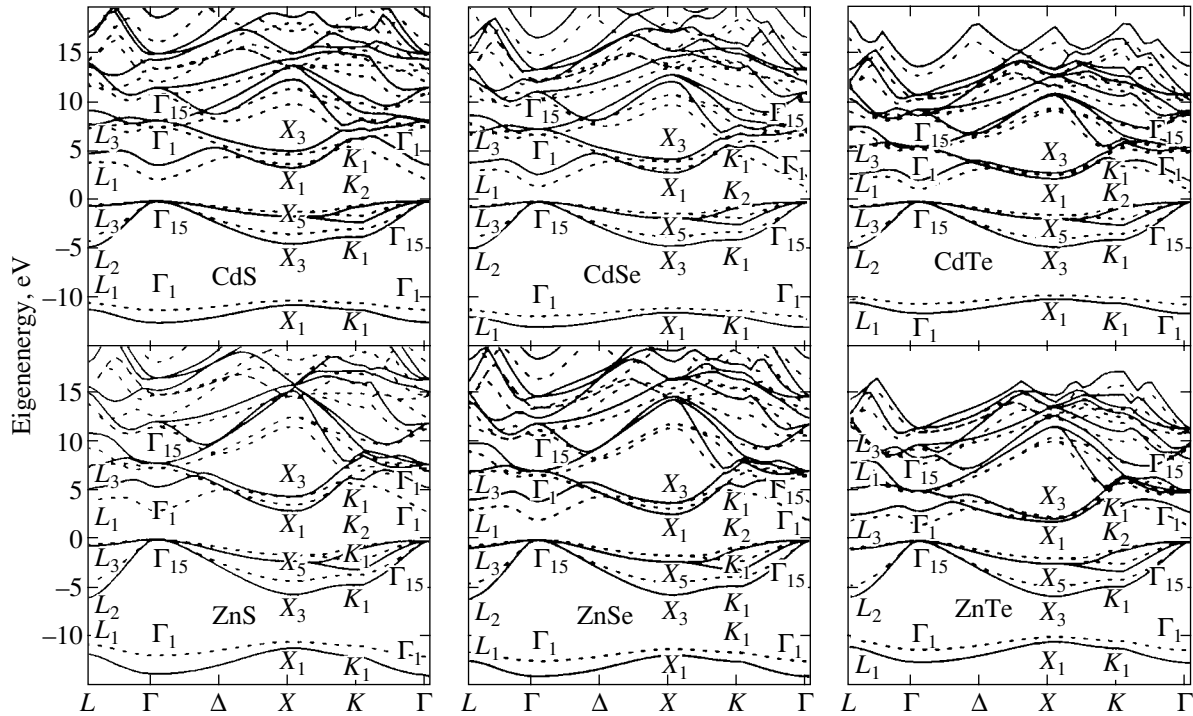
Fig. 1. Results of the band-structure calculations. Solid curves are calculated with theoretical lattice constants (a_0) and dashed curves with experimental ones (a_e).

and theoretical lattice constants are used in band-structure calculations, then the band gaps of all the II–VI compounds (except CdSe and CdTe) become indirect, with the valence-band maximum at point Γ and the conduction-band minimum at point X (see Table 2 and Fig. 1), which contradicts the experimental data [37, 38, 40]. This error is because of the big difference between the LDA lattice constants and the experimentally determined ones (see Table 1). If the experimental lattice constants are used in band-structure calculations, then eigenenergies (Table 2 and Fig. 1) are much more consistent with the LDA [25, 26] and GW [25] calculations.

It is well known that the inclusion of the d electrons of the atoms of Group-II in the valence complex causes strong p–d coupling of the upper valence band with d states, which results in a repulsion of the former upward and reduces the band gap [24–26, 29]. Our results in Table 2 and Fig. 2 are consistent with this statement. Furthermore, the energy levels of the d electrons (Γ_{12}^d and Γ_{15}^d) fall between the s and p valence bands, which is in good agreement with the calculations of Wang and Klein [13] for ZnS and ZnSe using a linear combination of Gaussian orbitals method with the LDA. However, the energies of the bands are much higher than the experimentally determined ones [30], which indicates an overestimation of the p–d coupling by the LDA, in agreement with the calculations in [13, 24–26, 29]. The Γ_{12}^d and Γ_{15}^d bands are almost dispersionless and very narrow. It indicates that these states

are well localized. Therefore, the above-mentioned overestimation is consistent with Wang and Klen's statement [13]: "…the more these lower states are localized (narrower bands), the larger the disagreement is…." Comparing Fig. 1 with Fig. 2, one can see that, due to the involvement of d electrons in the valence shell, the band gaps are significantly reduced for the II–VI compounds considered. Note that the difference between the eigenenergies calculated using the theoretical and the experimental lattice constants in Fig. 2 is smaller than that in Fig. 1. The small difference of the former is because the LDA and experimental lattice constants are close to each other.

Analysis of Table 2 (also, Fig. 1 and Fig. 2) shows that the band gaps calculated in this work using the experimental lattice constant and including the d electrons in the core are much bigger than those of previous ones calculated using the LDA [25] and smaller than those determined by the GW [25] approach using experimental lattice constants. Our calculated band gap for ZnS is also smaller than 3.55 eV [26]. However, our calculated band gaps, obtained with the d electrons included in the valence complex, are in good agreement with 1.02 eV for ZnTe, 0.47 eV for CdTe [24], and 1.84 eV for ZnS [26], which are much smaller than the experimental values.

The eigenvalues at some of the special k points for a number of the compounds considered is in general agreement with other LDA calculations (e.g., those by Huang and Ching [14] using a minimal basis semi–ab
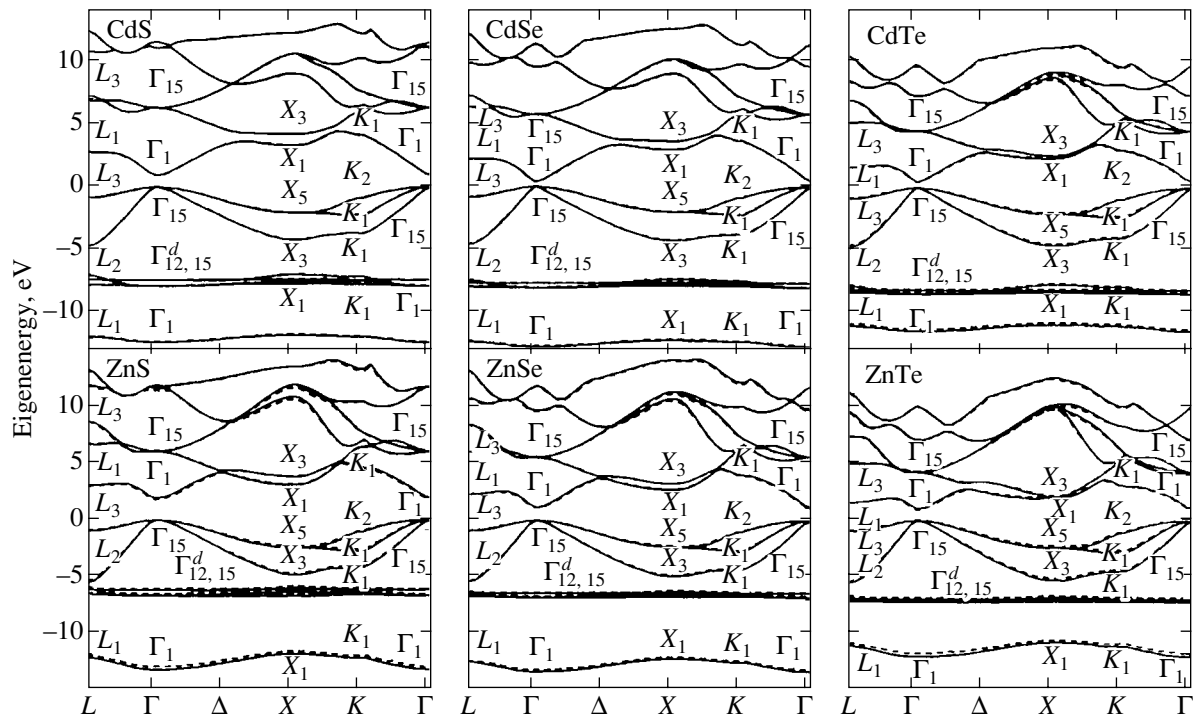
Fig. 2. Results of the band-structure calculations with the inclusion of the d electrons of Group-II atoms in the valence complex. Solid curves are calculated with theoretical lattice constants (ad_0) and dashed curves with experimental ones (ad_e).

initio approach and by Wang and Klein [13] using the LDA). However, the agreement is not systematic. Note that the discrepancies between the theoretical band gaps of different authors can be related to the accuracy of the LDA calculations; different parameters used to generate the pseudopotentials of the atoms of Group-II, III, V and VI; and different values of the E_{cut} and lattice constant.

The other important conclusions that can be derived from this comparative analysis is that, systematically, the band gaps (E_g) are underestimated and the energies of the semicore states are overestimated. However, this error, as discussed in Section 1, is not an artifact of numerical band-structure approximations, rather it is a failure of DFT.

3.3. Momentum Matrix Elements and Luttinger Parameters

Momentum matrix elements are the key parameters when discussing the optical properties of semiconductors. Therefore, to study the problem using ab initio band structure calculations is an important step. Our calculated results for E_p and E_p', and the Luttinger parameters γ_1^L, γ_2^L, and γ_3^L are given in Table 3 and Table 4 for the III–V and II–VI compounds, respectively.

Analysis of Tables 3 and 4 shows that the momentum matrix elements calculated in this study are much smaller than those found from $\mathbf{k} \cdot \mathbf{p}$ theory for all the semiconductors considered except AlP, ZnS and ZnSe for which good agreement was achieved. The small values of E_p can be related to the underestimation of the coupling of the valence-band maximum [20]. For InP our result agrees well with that of Fu, Wang, and Zunger [21, 44] calculated by the direct diagonalization method. In addition, $E_p' < E_p$ for all the semiconductors apart from GaSb, InAs, and InSb that have zero band gaps in the LDA calculations using experimentally determined lattice constants.

Momentum matrix elements calculated when the d electrons of Group-II atoms are kept in the core are larger than those found for the d electrons included in the valence complex. This indicates that the d electrons result in the underestimation of the coupling between the conduction band minimum and valence band maximum. The former approach gives better agreement with tight-binding and LMTO calculations [5] for ZnS, ZnSe, and ZnTe, and also with $\mathbf{k} \cdot \mathbf{p}$ calculations [2] for ZnS. However, for all the II–VI compounds considered other than ZnTe, the value of E_p' is much smaller than that calculated in [5], where it was found that the value of E_p' is comparable to that of E_p. Note that the momentum matrix element between the semicore Γ_{15}^d states and conduction band minimum (not shown in Table 4) is between 1 and 3 eV, which is smaller than E_p but

Table 3. Momentum matrix elements (eV) and Luttinger parameters for zinc-blende III–V compounds using the theoretical (a_0) and experimental (a_e) lattice constants

		E_p	E_p'	γ_1^L	γ_2^L	γ_3^L
AlP	a_0	17.183	0.015	3.696	0.826	1.454
	a_e	16.807	0.036	3.750	0.893	1.494
	$\mathbf{k} \cdot \mathbf{p}$ [2]	17.700		3.470	0.060	1.150
AlAs	a_0	15.678	0.144	5.203	1.526	2.179
	a_e	15.437	0.172	5.355	1.628	2.263
	[39]	21.100		3.45, 3.25	0.68, 0.64	1.29, 1.21
	$\mathbf{k} \cdot \mathbf{p}$ [2]	21.100		4.040	0.780	1.570
AlSb	a_0	14.548	0.592	5.810	1.659	2.401
	a_e	14.206	0.634	6.180	1.898	2.604
	$\mathbf{k} \cdot \mathbf{p}$ [2]	18.700		4.150	1.010	1.750
GaP	a_0	18.758	0.150	5.729	1.222	2.289
	a_e	17.496	0.366	6.517	1.872	2.672
	[39]	22.200		4.050	0.490	1.250
	$\mathbf{k} \cdot \mathbf{p}$ [2]	22.200		4.200	0.980	1.660
GaAs	a_0	17.189	0.440	10.336	3.526	4.479
	a_e	16.136	0.634	18.198	7.674	8.493
	[39]	25.700		6.80–7.20	2.10–2.50	1.00–2.90
	$\mathbf{k} \cdot \mathbf{p}$ [2]	25.700		7.650	2.410	3.280
	$\mathbf{k} \cdot \mathbf{p}$ [2], TB [45]	22.500	0.025	7.070	2.400	3.050
	Experiment [17]	22.53–28.9	3.55–6.0	5.64–7.21	1.35–2.49	2.49–3.09
	Experiment [18]	27.860	2.36	4.80–8.56	1.22–2.90	1.85–3.74
	LDA [15]	15.820	2.27	9.270	3.120	4.010
GaSb	a_0	15.726	0.997	16.291	6.305	7.371
	a_e	0.000	8.540	115.200	56.033	56.933
	$\mathbf{k} \cdot \mathbf{p}$ [2]	22.400		11.800	4.030	5.260
	[39]	25.00, 26.1		13.10, 13.30	4.40, 4.50	5.70, 6.00
InP	a_0	15.456	0.048	6.638	3.033	2.760
	a_e	14.314	0.205	9.768	3.836	4.423
	[39]	17.000		4.95–5.15	0.94–1.65	1.62–2.35
	$\mathbf{k} \cdot \mathbf{p}$ [2]	20.400		6.280	2.080	2.760
InAs	a_0	14.427	0.169	19.481	8.428	9.171
	a_e	0.000	7.132	33.807	15.819	16.427
	$\mathbf{k} \cdot \mathbf{p}$ [2]	22.200		19.670	8.370	9.290
InSb	a_0	13.866	0.454	24.259	10.681	11.504
	a_e	0.000	7.152	23.493	10.545	11.220
	[39]	21.200		33.50, 40.10	14.50, 18.10	15.70, 19.20
	$\mathbf{k} \cdot \mathbf{p}$ [2], TB [45]	23.100		35.080	15.640	16.910

about 10 times bigger than those between the other remote bands for all the II–VI compounds considered. This factor can be related to the LDA overestimation of the influence of the valence band semicore d states. Matrix elements between the lowest conduction band Γ_1^c and valence band Γ_{12}^d, and the remote conduction band states Γ_1^c and Γ_{12}^c is zero, which is related to the symmetry properties of the crystal.

Luttinger parameters calculated in this study for the III–V compounds in Table 3 are much smaller than those found by $\mathbf{k} \cdot \mathbf{p}$ theory or experiments, though the order of magnitude is the same. For II–VI semiconduc-

Table 4. Momentum matrix elements (eV) and Luttinger parameters for II–VI semiconductors with d electrons of Group-II atoms included in the core (a_0, a_e) and in the valence complex (ad_0, ad_e) using the theoretical (a_0, ad_0) and experimental (a_e, ad_e) lattice constants. The results are compared to calculations within other methods, such as TBLMTO [5] and $\mathbf{k} \cdot \mathbf{p}$ [2, 23]

		E_p	E_p'	γ_1^L	γ_2^L	γ_3^L
ZnS	a_0	19.649	0.008	3.158	0.746	1.262
	a_e	14.735	0.279	2.981	0.973	1.278
	ad_0	12.262	0.232	4.113	1.160	1.641
	ad_e	12.013	0.301	4.143	1.241	1.686
	TBLMTO [5]	24.882	20.998	2.120	0.510	1.560
	TBLMTO [5]	15.295	6.708	1.280	0.090	1.140
	$\mathbf{k} \cdot \mathbf{p}$ [2]	20.400		2.540	0.750	1.090
ZnSe	a_0	16.961	0.048	3.954	1.079	1.635
	a_e	12.843	0.545	4.238	1.542	1.882
	ad_0	11.358	0.484	6.465	2.371	2.831
	ad_e	11.146	0.544	6.817	2.530	3.008
	[37]			4.300	1.140	1.840
	$\mathbf{k} \cdot \mathbf{p}$ [23]	23.000				
	TBLMTO [5]	16.230	9.835	3.210	0.750	2.000
	$\mathbf{k} \cdot \mathbf{p}$ [2]	24.200		3.770	1.240	1.670
ZnTe	a_0	16.075	0.507	4.327	1.132	1.759
	a_e	12.758	1.062	4.835	1.721	2.131
	ad_0	12.272	0.907	7.215	2.511	3.123
	ad_e	11.820	1.020	7.790	2.897	3.451
	TBLMTO [5]	19.667		3.440	0.590	2.030
	[37]			3.900	0.600	0.900
	[37]			3.900	0.830	1.300
	[37]			4.000	0.830	1.300
	[37]				0.800	1.700
	$\mathbf{k} \cdot \mathbf{p}$ [2]	19.100		3.740	1.070	1.640
CdS	a_0	15.356	0.000	2.721	0.841	1.152
	a_e	11.631	0.195	2.647	0.975	1.181
	ad_0	9.301	0.219	5.101	1.880	2.224
	ad_e	9.273	0.228	5.121	1.897	2.238
	TBLMTO [5]			3.440	0.970	2.150
	TBLMTO [5]			2.200	0.350	1.530
	$\mathbf{k} \cdot \mathbf{p}$ [23]	21.000				
CdSe	a_0	13.563	0.036	3.265	1.162	1.443
	a_e	10.125	0.374	3.806	1.515	1.735
	ad_0	8.670	0.384	11.694	5.144	5.511
	ad_e	8.600	0.405	12.160	5.394	5.752
	TBLMTO [5]			4.40	1.600	2.680
	$\mathbf{k} \cdot \mathbf{p}$ [23]	20.000				
CdTe	a_0	13.600	0.256	3.862	1.258	1.664
	a_e	10.732	0.663	4.353	1.709	1.982
	ad_0	9.735	0.628	10.072	4.207	4.652
	ad_e	9.488	0.697	11.208	4.831	5.245
	TBLMTO [5]	21.066	5.098	4.340	1.600	2.660
	[37]			5.300	1.700	2.000
	[37]			4.110	1.080	1.950
	$\mathbf{k} \cdot \mathbf{p}$ [23]	18.500				
	$\mathbf{k} \cdot \mathbf{p}$ [2]	20.700		5.290	1.890	2.460

Table 5. Effective masses (in units of the free-electron mass m_0) for zinc-blende III–V compounds calculated using the theoretical (a_0) and experimentally determined (a_e) lattice constants. The results have been compared to those calculated within pseudopotential [46], $\mathbf{k} \cdot \mathbf{p}$ [17, 18, 45] and semi–ab initio [14] theories, and to experimental data [17, 18, 45, 46]

		m_c^{001}	m_c^{011}	m_c^{111}	m_{hh}^{001}	m_{hh}^{011}	m_{hh}^{111}	m_{lh}^{001}	m_{lh}^{011}	m_{lh}^{111}
AlP	a_0	0.176	0.176	0.176	0.489	6.272, 0.490	1.270	0.187	0.139	0.128
	a_e	0.170	0.170	0.170	0.509	6.138, 0.509	1.310	0.181	0.137	0.126
	[14]				0.513		1.372	0.211		0.145
AlAs	a_0	0.115	0.115	0.115	0.465	5.199, 0.465	1.183	0.121	0.098	0.092
	a_e	0.110	0.110	0.110	0.476	5.142, 0.476	1.206	0.116	0.095	0.090
	[14]				0.409		1.022	0.153		0.109
	[46]	0.152			0.457		1.087	0.200		0.161
	Experiment [46]	0.150			0.478		1.149	0.208		0.166
	LDA [9]		0.122			0.480			0.129	
	Experiment [9]		0.124			0.491			0.153	
AlSb	a_0	0.110	0.110	0.110	0.401	3.746, 0.401	0.992	0.110	0.088	0.083
	a_e	0.100	0.100	0.100	0.419	3.769, 0.419	1.029	0.100	0.083	0.078
	[14]				0.336		0.872	0.123		0.091
GaP	a_0	0.128	0.128	0.128	0.305	2.444, 0.305	0.731	0.122	0.090	0.083
	a_e	0.100	0.100	0.100	0.361	2.687, 0.361	0.853	0.097	0.079	0.074
	[14]				0.419		0.997	0.160		0.113
GaAs	a_0	0.058	0.057	0.058	0.304	2.353, 0.305	0.726	0.058	0.049	0.047
	a_e	0.030	0.030	0.030	0.351	2.551, 0.351	0.826	0.030	0.028	0.027
	[14]				0.395		0.934	0.089		0.072
	[15]	0.067			0.460		0.950	0.085		0.077
	Experiment [17]				0.340–0.475		0.450–1.030	0.082–0.120		0.070–0.082
	$\mathbf{k} \cdot \mathbf{p}$ [18]				0.340–0.800		0.520–4.000	0.082–0.142		0.075–0.120
GaSb	a_0	0.035	0.035	0.036	0.272	2.074, 0.272	0.646	0.035	0.031	0.030
	a_e	0.004	0.006	0.008	0.219	2.274, 0.319	0.747	0.004	0.006	0.008
	[14]				0.231		0.551	0.052		0.047
InP	a_0	0.095	0.095	0.095	0.389	2.570, 0.389	0.895	0.093	0.078	0.074
	a_e	0.058	0.058	0.058	0.477	2.979, 0.477	1.084	0.057	0.052	0.051
	LDA [42]	0.570			0.430		0.970	0.057		
	SLDA [42]	0.060			0.400		0.900	0.057		
	SEPM [42]	0.095			0.470		1.030	0.097		
	Experiment [42]	0.079, 0.081			0.520, 0.610		0.630, 0.950	0.104, 0.118		
InAs	a_0	0.028	0.028	0.028	0.381	2.524, 0.381	0.878	0.028	0.026	0.026
	a_e	0.015	0.017	0.018	0.461	2.885, 0.461	1.048	0.015	0.016	0.017
	EPM [47]				0.480			0.040		
	LDA [10]	0.094		0.112	0.353			0.046		
	sX [10]	0.022		0.021	0.388			0.025		
	Experiment [10]	0.023			0.410			0.026		
	$\mathbf{k} \cdot \mathbf{p}$ [2]	0.023			0.410			0.026		
	Experiment [2]	0.024			0.410			0.026		
InSb	a_0	0.022	0.023	0.023	0.345	2.333, 0.345	0.799	0.022	0.021	0.021
	a_e	0.023	0.024	0.025	0.416	2.638, 0.416	0.949	0.022	0.023	0.024

Table 6. Effective masses (in units of the free-electron mass m_0) for II–VI semiconductors including the d electrons of atoms of Group-II in the core (a_0, a_e) and in the valence complex (ad_0, ad_e), and using the LDS (a_0, ad_0) and experimentally determined (a_e, ad_e) lattice constants. In [2, 37] all the effective masses (except CdTe and m_c^{011} for ZnS, [37]) are given without specific directions and are determined experimentally [37]

		m_c^{001}	m_c^{011}	m_c^{111}	m_{hh}^{001}	m_{hh}^{011}	m_{hh}^{111}	m_{lh}^{001}	m_{lh}^{011}	m_{lh}^{111}
ZnS	a_0	0.193	0.193	0.193	0.601	8.463, 0.601	1.578	0.215	0.161	0.149
	a_e	0.183	0.183	0.183	0.966	8.938, 0.961	2.350	0.203	0.171	0.162
	ad_0	0.145	0.145	0.145	0.557	2.884, 0.556	1.203	0.155	0.127	0.119
	ad_e	0.142	0.141	0.141	0.602	3.071, 0.602	1.297	0.151	0.126	0.119
	Experiment [37]	0.340	0.184			1.760, 1.121			0.230	0.169
	k · p [2]		0.280							
ZnSe	a_0	0.146	0.146	0.146	0.557	7.505, 0.561	1.462	0.164	0.129	0.120
	a_e	0.126	0.126	0.126	0.866	7.550, 0.867	2.113	0.137	0.120	0.115
	ad_0	0.083	0.084	0.084	0.581	3.651, 0.559	1.246	0.089	0.078	0.075
	ad_e	0.081	0.081	0.081	0.569	3.078, 0.571	1.248	0.084	0.075	0.073
	Experiment [37]	0.142	0.147	0.160						
	Experiment [40]	0.130	0.170	0.570	0.750					
	k · p [2]		0.140							
	[14]				1.814		0.784	0.191		0.147
ZnTe	a_0	0.146	0.147	0.147	0.485	5.501, 0.484	1.236	0.152	0.118	0.110
	a_e	0.118	0.118	0.118	0.717	5.975, 0.719	1.742	0.121	0.105	0.101
	ad_0	0.081	0.081	0.081	0.456	2.800, 0.456	1.032	0.082	0.071	0.068
	ad_e	0.073	0.073	0.073	0.501	2.988, 0.501	1.126	0.074	0.066	0.063
	Experiment [37]	0.122	0.128	0.130						
	Experiment [40]	0.130			0.600					
	k · p [2]		0.180							
	[14]				0.541		1.354	0.155		0.119
CdS	a_0	0.196	0.197	0.197	0.962	12.800, 0.953	2.400	0.227	0.184	0.173
	a_e	0.191	0.190	0.190	1.433	12.621, 1.433	3.499	0.218	0.192	0.184
	ad_0	0.108	0.108	0.108	0.745	3.249, 0.745	1.532	0.113	0.101	0.097
	ad_e	0.107	0.107	0.107	0.754	3.285, 0.754	1.551	0.112	0.101	0.097
	Experiment [40]		0.140		0.510					
	[14]				0.929		1.935	0.201		0.161
CdSe	a_0	0.079	0.104	0.116	1.063	46.105, 0.943	2.643	0.179	0.147	0.139
	a_e	0.134	0.133	0.133	1.289	8.295, 1.309	2.982	0.146	0.133	0.129
	ad_0	0.045	0.045	0.045	0.711	3.282, 0.712	1.491	0.045	0.043	0.043
	ad_e	0.043	0.043	0.043	0.729	3.355, 0.729	1.524	0.044	0.042	0.041
	Experiment [37]	0.11								
	Experiment [40]		0.110		0.44					
CdTe	a_0	0.145	0.146	0.146	0.743	7.910, 0.742	1.874	0.157	0.132	0.125
	a_e	0.122	0.122	0.122	1.070	8.542, 1.070	2.567	0.129	0.117	0.113
	ad_0	0.054	0.054	0.054	0.603	3.110, 0.603	1.304	0.054	0.051	0.050
	ad_e	0.047	0.048	0.048	0.647	3.292, 0.647	1.393	0.048	0.045	0.045
	Experiment [37]	0.094	0.096	0.095	0.720	0.810	0.840	0.130	0.120	0.120
	Experiment [37]	0.099								
	Experiment [40]		0.90		0.720	0.840		0.120		
	k · p [2]		0.096							
	[14]				0.478		1.114	0.125		0.095

tors, we found that the involvement of *d* electrons in the core significantly reduces the Luttinger parameters compared to those with *d* electrons in the valence complex (see Table 4). However, the former approach gives better agreement with $\mathbf{k} \cdot \mathbf{p}$ theory [2], and with tight-binding and linear muffin-tin-orbital (TBLMTO) calculations [5]. This analysis indicates that, from LDA calculations, one can sometimes attain the correct momentum matrix elements and Luttinger parameters; however, this can not be achieved systematically.

3.4. Effective Masses

Carrier effective masses are one of the important parameters in any discussion of transport phenomena, exciton effects, electron–hole liquids, and so on in semiconductors. They are usually determined by cyclotron resonance, electroreflectance measurements or from analysis of transport data. In this section we present the results of our calculations of electron effective masses at the conduction band minimum and hole effective masses at the valence band maximum. The results for III–V and II–VI compounds are given in Table 5 and Table 6, respectively. For the indirect gap semiconductors AlP, AlAs, AlSb, and GaP, m_c is usually discussed for the conduction band minimum at Γ and points other than Γ (say X or L). In this study, we consider all effective masses only for point Γ.

Analysis of Tables 5 and 6 shows that the effective masses of conduction band electrons are isotropic, while those of the holes are anisotropic. The effective masses for heavy-holes (m_{hh}) and light-holes (m_{lh}) correspond to the splitting of the Γ_{15}^v state into double and single degenerate bands, respectively. Since we have disregarded spin–orbit coupling, the split-off mass band is not discussed. Analysis of Table 5 shows that conduction-band effective masses for AlP, AlSb, GaP, GaSb, and InSb are much smaller than the $m_c = 0.25, 0.18, 0.17, 0.22$, and 0.13 calculated by $\mathbf{k} \cdot \mathbf{p}$ theory [2]. One can also see that conduction-band effective masses calculated using the LDA lattice constant are closer to experimental data than those calculated using the experimental lattice constant. Note that all the effective masses for AlP, AlAs, AlSb, and InSb using the theoretical and experimentally determined lattice constants do not differ from each other very much, while the difference is significant for the other III–V semiconductors studied.

Analysis of Table 5 shows that the values of m_{hh}^{001} and m_{hh}^{111} for AlAs, GaAs, InP, and InAs calculated in this study agree well with previous calculations and experimental data, while such an agreement was not achieved for m_{lh}^{001} and m_{lh}^{111}. Due to the lack of experimental or calculated data, we could not make such a comparison for other semiconductors and for effective masses in other directions. For InP, InAs, and InSb,

note that not only the band gaps but also conduction-band effective masses are overestimated. This indicates that there is a correlation between changes in the band gap and the conduction-band effective mass, which is qualitatively consistent with the $\mathbf{k} \cdot \mathbf{p}$ theory (see, e.g., [2]). Moreover, distinct from Fiorentini and Baldereschi [8, 9], none of the conduction-band effective masses for III–V compounds apart from AlAs agree with the experimental data.

Analysis of Table 6 shows that the effective masses of all the II–VI compounds calculated when the *d* electrons are kept in the core is bigger than those found when including the *d* electrons in the valence complex. It indicates that the semicore *d* electrons result not only in an underestimation of the band and coupling between the valence band maximum and conduction band minimum, but also change the dispersion around point Γ. Our calculated values of the light-hole effective masses (m_{lh}) are in good agreement with experimental data for ZnS and CdTe. Due to the lack of theoretical or experimental data we could not make such a comparison for the other II–VI compounds. Calculated heavy-hole effective masses (m_{hh}) differ significantly from those of [2, 37, 40] for all the II–VI compounds considered other than CdTe. For the latter, good agreement is achieved if the theoretical lattice constant is used.

The effective masses for all the compounds considered agree somewhat with those calculated by Huang and Ching [14] using a minimal basis semi–ab initio approach and by Wang and Klein [13] using the LDA, but the agreement is not systematic. Based on the above analysis, one can say that LDA calculations can sometimes provide the correct values of conduction or valence-band effective masses in some of the specific directions. However, it is not systematic.

4. CONCLUSION

In summary, band-structure calculations were performed for III–V and II–VI semiconductors with a zinc-blende structure. By a search of the total energy minimum, lattice constants were found that differ from the experimentally determined ones by <3% for III–V compounds, and by 1.5 and 7% for the II–VI semiconductors with the *d* electrons of Group-II atoms included into the valence shell and into the core, respectively.

Band parameters calculated within the LDA correctly have a tendency to be smaller than those determined experimentally or calculated theoretically within the $\mathbf{k} \cdot \mathbf{p}$, tight-binding, or semi-empirical methods. From this point of view, our results are in general agreement with those obtained using the other ab initio codes.

The difference of the calculated direct band gaps for III–V compounds are in the range from 6.5 to 66% for theoretical lattice constants and from 15 to 100% for experimental lattice constants. The difference for the II–VI semiconductors with the *d* electrons of Group-II atoms included in the core is in the range from 30 to

47% for theoretical lattice constant and from 14 to 28% for experimental lattice constant. If the d electrons are included in the valence complex, then the error in the calculation of the band gap becomes significant due to $p–d$ repulsion.

The momentum matrix elements E_p calculated in this study are smaller than those obtained within the $\mathbf{k} \cdot \mathbf{p}$ theory [2], since the latter is known to be closer to experimental data. For III–V compounds, the difference between the values of E_p obtained within the two theories is in the range from 2.9 to 35% for the theoretical lattice constant and from 21 to 38% for experimentally determined lattice constants. For II–VI compounds with the d electrons of Group-II atoms included in the core, the difference is in the range from 3.7 to 34.3% for the theoretical lattice constant and from 27.8 to 48.1% for the experimentally determined lattice constant. Involvement of the d electrons in the valence complex increases the error in the calculation of E_p.

The effective masses of conduction band electrons were found to be isotropic, while those of holes were anisotropic. Calculated m_c for the III–V semiconductors differed from experimentally determined m_c by 13 to 23% for the theoretical lattice constant and from 26 to 55% for the experimental lattice constant. For II–VI compounds with the d electrons of Group-II atoms included in the core, the difference of the calculated m_c from experimentally determined m_c is in the range from 8 to 54% for the theoretical lattice constant, while that for the experimental lattice constant is in the range from 2 to 46%. We found that the effective masses of all the $A^{II}B^{VI}$ compounds calculated when the d electrons are kept in the core are larger than those found when including the d electrons in the valence complex. This indicates that the semicore d electrons not only result in an underestimation of band gaps and coupling between the valence band maximum and conduction band minimum, but also change the dispersion around point Γ. Furthermore, conduction-band effective masses calculated using the LDA lattice constant are closer to experimental data than those calculated using the experimental lattice constant. The effective masses for all the compounds considered partially agree with those calculated by Huang and Ching [14] using a minimal basis semi–ab initio approach and by Wang and Klein [13], but the agreement is not systematic.

We found that the correctness of the LDA band parameters for all the compounds considered is not systematic. Comparing the LDA band parameters calculated using the LDA and using experimental lattice constants, we conclude that the latter is more preferable to use for LDA band-structure calculation. We showed that consideration of the d electrons of Group-II atoms in the core can give more correct band parameters for II–VI compounds. We found that involvement of the d electrons of Group-II atoms in the valence shell in the LDA band-structure calculations results in a decrease of band gaps; a increase of lattice constants; a decrease

of momentum matrix elements; an increase of Luttinger parameters; and a decrease of electron, heavy-hole and light-hole effective masses in all directions. In this case, only the equilibrium lattice constant can be determined with a high accuracy, while all the other band parameters are inaccurate.

REFERENCES

1. L. J. Sham and M. Schlüter, Phys. Rev. Lett. **51**, 1888 (1983).
2. P. Lawaetz, Phys. Rev. B **4**, 3460 (1971).
3. M. Willatzen, M. Cardona, and N. E. Christensen, Phys. Rev. B **50**, 18054 (1994).
4. M. Willatzen, M. Cardona, and N. E. Christensen, Phys. Rev. B **51**, 13150 (1995).
5. M. Willatzen, M. Cardona, and N. E. Christensen, Phys. Rev. B **51**, 17992 (1995).
6. L. C. Lew Yan Voon, M. Willatzen, and M. Cardona, Phys. Rev. B **53**, 10703 (1996).
7. L. C. Lew Yan Voon, S. Karazhanov, and W. A. Harrison, Phys. Rev. B **66**, 235211 (2002).
8. V. Fiorentini and A. Baldereschi, J. Phys.: Condens. Matter **4**, 5967 (1992).
9. V. Fiorentini, Phys. Rev. B **46**, 2086 (1992).
10. C. B. Geller, W. Wolf, S. Picozzi, *et al.*, Appl. Phys. Lett. **79**, 368 (2001).
11. L.-W. Wang and A. Zunger, Phys. Rev. B **51**, 17398 (1995).
12. E. O. Kane, Phys. Rev. B **4**, 1910 (1971).
13. C. S. Wang and B. M. Klein, Phys. Rev. B **24**, 3393 (1981).
14. M.-Z. Huang and W. Y. Ching, J. Phys. Chem. Solids **46**, 977 (1985).
15. R. Winkler, in *Proceedings of 24th International Conference on the Physics of Semiconductors*, Ed. by D. Gershoni (World Sci., Jerusalem, 1998).
16. H. Kageshima and K. Shiraishi, Phys. Rev. B **56**, 14985 (1997).
17. T. E. Ostromek, Phys. Rev. B **54**, 14467 (1996).
18. P. Pfeffer and W. Zawadzki, Phys. Rev. B **53**, 12813 (1996).
19. Z. H. Levine and D. C. Allan, Phys. Rev. Lett. **63**, 1719 (1989).
20. A. L. Efros and M. Rosen, Appl. Phys. Lett. **73**, 1155 (1998).

21. H. Fu, L.-W. Wang, and A. Zunger, Appl. Phys. Lett. **71**, 3433 (1997).
22. T. Nakashima, C. Hamaguchi, J. Komeno, and M. Ozeki, J. Phys. Soc. Jpn. **54**, 725 (1985).
23. C. Hermann and C. Weisbuch, Phys. Rev. B **15**, 823 (1977).
24. S.-H. Wei and A. Zunger, Phys. Rev. B **37**, 8958 (1988).
25. O. Zakharov, A. Rubio, X. Blase, *et al.*, Phys. Rev. B **50**, 10780 (1994).
26. P. Schröer, P. Krüger, and J. Pollman, Phys. Rev. B **47**, 6971 (1993).
27. M. Rohlfing, P. Krüger, and J. Pollman, Phys. Rev. B **56**, R7065 (1997).
28. M. Rohlfing, P. Krüger, and J. Pollman, Phys. Rev. B **57**, 6485 (1998).
29. W. Luo, S. Ismail-Beigi, M. L. Cohen, and S. G. Louie, Phys. Rev. B **66**, 195215 (2002).
30. L. Ley, R. A. Pollak, F. R. McFeely, *et al.*, Phys. Rev. B **9**, 600 (1974).
31. N. Trouillier and J. L. Martins, Phys. Rev. B **43**, 1993 (1991).
32. L.-W. Wang, *Planewave Total Energy Code (PEtot)*, http://www.nersc.gov/~linwang/PEtot/PEtot.html (2001).
33. J. P. Perdew and A. Zunger, Phys. Rev. B **23**, 5048 (1981).
34. D. M. Ceperley and B. J. Alder, Phys. Rev. Lett. **45**, 566 (1980).
35. M. C. Payne, M. P. Teter, D. C. Allan, *et al.*, Rev. Mod. Phys. **64**, 1045 (1992).
36. S. K. Pugh, D. J. Dugdale, S. Brand, and R. A. Abram, Semicond. Sci. Technol. **14**, 23 (1999).
37. *Numerical Data and Functional Relationships in Science and Technology. New Series. Group III: Crystal and Solid State Physics. Semiconductors*, Suppl. and Extens., Vol. III/17. *Intrinsic Properties of Group IV Elements and III–V, II–VI and I–VII Compounds*, Ed. by O. Madelung and M. Schulz (Springer, Berlin, 1982), Vol. 22a.
38. N. K. Abrikosov, V. B. Bankina, L. V. Portskaya, L. E. Shelimova, and E. V. Skudnova, *Semiconducting II–VI, IV–VI, and V–VI Compounds* (Plenum, New York, 1969).
39. *Numerical Data and Functional Relationships in Science and Technology. New Series. Group III: Crystal and Solid State Physics. Semiconductors. Physics of Group IV Elements and III–V Compounds*, Ed. by O. Madelung, M. Schulz, and H. Weiss (Springer, Berlin, 1982), Vol. 17a.
40. *Data in Science and Technology. Semiconductors: Other than Group IV Elements and III–V Compounds*, Ed. by O. Madelung (Springer, Berlin, 1992).
41. S.-H. Wei and A. Zunger, Phys. Rev. B **39**, 3279 (1989).
42. H. Fu and A. Zunger, Phys. Rev. B **55**, 1642 (1997).
43. M. L. Cohen and J. R. Chelikowsky, *Electronic Structure and Optical Properties of Semiconductors* (Springer, Berlin, 1988).
44. H. Fu, L.-W. Wang, and A. Zunger, Appl. Phys. Lett. **73**, 1157 (1998).
45. N. Cavassilas, F. Aniel, K. Boujdaria, and G. Fishman, Phys. Rev. B **64**, 115207 (2001).
46. D. M. Wood and A. Zunger, Phys. Rev. B **53**, 7949 (1996).
47. L.-W. Wang, J. Kim, and A. Zunger, Phys. Rev. B **59**, 5678 (1999).